

SESAMI Web: An Accessible Interface for Surface Area Prediction of Materials from Adsorption Isotherms

Gianmarco G. Terrones¹, Yu Chen², Archit Datar³, Li-Chiang Lin⁴, Heather J. Kulik^{1,5}, and Yongchul G. Chung²✉

¹ Department of Chemical Engineering, Massachusetts Institute of Technology, USA ² School of Chemical Engineering, Pusan National University, South Korea ³ William G. Lowrie Department of Chemical and Biomolecular Engineering, The Ohio State University, USA ⁴ Department of Chemical Engineering, National Taiwan University, Taiwan ⁵ Department of Chemistry, Massachusetts Institute of Technology, USA ✉ Corresponding author

DOI: [10.xxxxxx/draft](https://doi.org/10.xxxxxx/draft)

Software

- [Review](#)
- [Repository](#)
- [Archive](#)

Editor: [Open Journals](#)

Reviewers:

- [@openjournals](#)

Submitted: 01 January 1970

Published: unpublished

License

Authors of papers retain copyright and release the work under a Creative Commons Attribution 4.0 International License ([CC BY 4.0](#)).

Statement of need

Surface area determination is important for the evaluation of a porous material's viability in applications ranging from catalysis to separations to gas storage. The most widely used approach for the evaluation of a material's specific surface area, i.e. surface area per unit mass, is Brunauer-Emmett-Teller (BET) theory ([Brunauer et al., 1938](#)). Given the adsorption isotherm of a gas in an adsorbent, one can use BET theory to determine the specific surface area of the adsorbent upon identification of an appropriate linear region in the isotherm. This procedure is sometimes automatically performed by the software program that comes with the commercial adsorption apparatus that measures the adsorption isotherm. Unfortunately, the linear region selection is a large source of variability in BET-calculated areas. In addition, for certain types of isotherms, automatic selection of the linear region by the commercial software sometimes fails. As a result, many researchers perform the analyses manually on a spreadsheet, which can become time-consuming and nearly impossible for some types of isotherms ([Osterrieth et al., 2022](#)). These challenges have motivated the development of programs for the automated determination of BET areas ([Datar et al., 2020](#); [Iacomini & Llewellyn, 2019](#); [Osterrieth et al., 2022](#); [Sadeghi et al., 2020](#); [Sinha et al., 2019](#)). Furthermore, shortcomings of BET as a tool for surface area calculation, such as its relatively poor performance in treating high surface area materials with multimodal pore sizes ([Gómez-Gualdrón et al., 2016](#); [Wang et al., 2015](#)), have led to the development of alternate methods for surface area calculation from isotherms ([Datar et al., 2020](#); [Sinha et al., 2019](#)).

Summary

In contrast to previously developed programs which require use of the command line ([Iacomini & Llewellyn, 2019](#); [Osterrieth et al., 2022](#)) and familiarity with Python ([Datar et al., 2020](#); [Iacomini & Llewellyn, 2019](#); [Sinha et al., 2019](#)), the SESAMI web interface allows a user to generate surface area predictions on their web browser by uploading isotherm data. The website facilitates access to the previously developed SESAMI models (SESAMI 1 and 2) for porous material surface area prediction ([Datar et al., 2020](#); [Sinha et al., 2019](#)) and has been tested by experimental groups. The motivation for this interface is to lower the barrier of entry for research groups seeking to use SESAMI code, which was previously packaged in Python and Jupyter Notebook scripts.

SESAMI 1 applies computational routines to identify suitable linear regions of adsorption

The SESAMI web interface has extensive error handling and clearly alerts users of issues with their adsorption isotherm data. For example, it alerts the user if no ESW minima is found by SESAMI 1 or if the data is incompatible with SESAMI 2 code due to data sparsity in certain pressure regions. As shown in Figure 1, the interface displays SESAMI 1 calculation results including information on the chosen linear region, namely the satisfied Rouquerol criteria (J. Rouquerol et al., 2007; Jean Rouquerol et al., 2013), the pressure range and number of data points in the region, and the coefficient of determination. The interface also displays intermediate SESAMI 1 values for surface area calculation, namely the BET constant, C , and the monolayer adsorption loading, q_m . Furthermore, the SESAMI web interface allows the user to download figures generated by SESAMI 1 that indicate, among other things, the chosen linear monolayer loading regions by the BET and BET+ESW approaches as well as the excess sorption work plot (Figure 1). The user can convert output from commercial equipment to AIF format and upload the converted data to the interface for analysis. The SESAMI web interface is publicly available at <https://sesami-web.org/>, and source code is available at https://github.com/hjkgp/SESAMI_web.

a)	SESAMI 1.0 (BET) results are: BET area = 2430.9 m ² /g C = 201.1 q _m = 28.42 mol/kg Rouquerol consistency criteria 1 and 2: Yes Rouquerol consistency criterion 3: Yes Rouquerol consistency criterion 4: Yes Number of points in linear region: 9 Lowest pressure of linear region: 3500 Pa Highest pressure of linear region: 8000 Pa R ² of linear region: 0.9996	SESAMI 1.0 (BET+ESW) results are: BET area = 2346.7 m ² /g C = 248.1 q _m = 27.44 mol/kg Rouquerol consistency criteria 1 and 2: Yes Rouquerol consistency criterion 3: No Rouquerol consistency criterion 4: Yes Number of points in linear region: 9 Lowest pressure of linear region: 600 Pa Highest pressure of linear region: 1500 Pa R ² of linear region: 0.9985
b)	SESAMI 2.0 (LASSO) surface area prediction is: 2099.1 m ² /g	

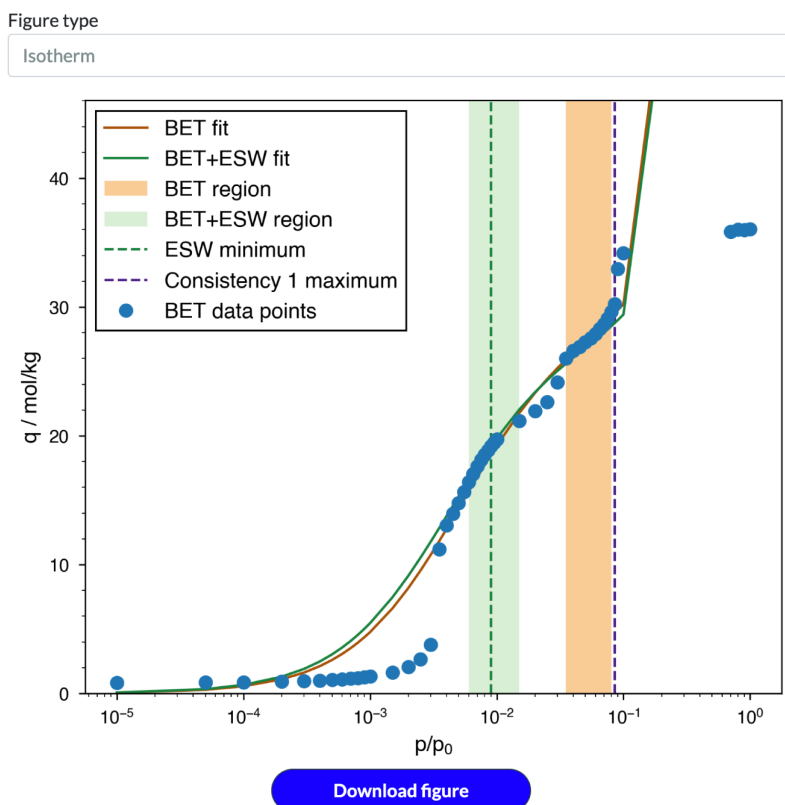


Figure 1: Information displayed by the SESAMI web interface after a calculation has been run. a) Interface printout of information on the SESAMI 1 chosen linear regions, and SESAMI 1 and 2 calculation results. b) Figure download functionality for figures detailing SESAMI 1 calculation.

71 Benchmarking

72 To assess the performance of SESAMI code in predicting surface areas from isotherms, we
 73 benchmarked the SESAMI routines against other similar programs for 13 simulated and 9
 74 experimental N₂ isotherms obtained at 77 K for 14 metal-organic frameworks, some of which
 75 are shown in Figure 2. Simulated isotherms were obtained from Grand Canonical Monte
 76 Carlo (GCMC) simulations using RASPA open-source software (Dubbeldam et al., 2016),
 77 and experimental adsorption isotherms were obtained from the experimental data reported

78 by Islamoglu and coworkers (Islamoglu et al., 2022). The data were then used to calculate
79 the surface areas from the SESAMI website, BETSI (Osterieth et al., 2022; Rampersad et
80 al., 2020), pyGAPS (Iacomini, 2019; Iacomini & Llewellyn, 2019), and BEaTmap (Sadeghi et al.,
81 2020).

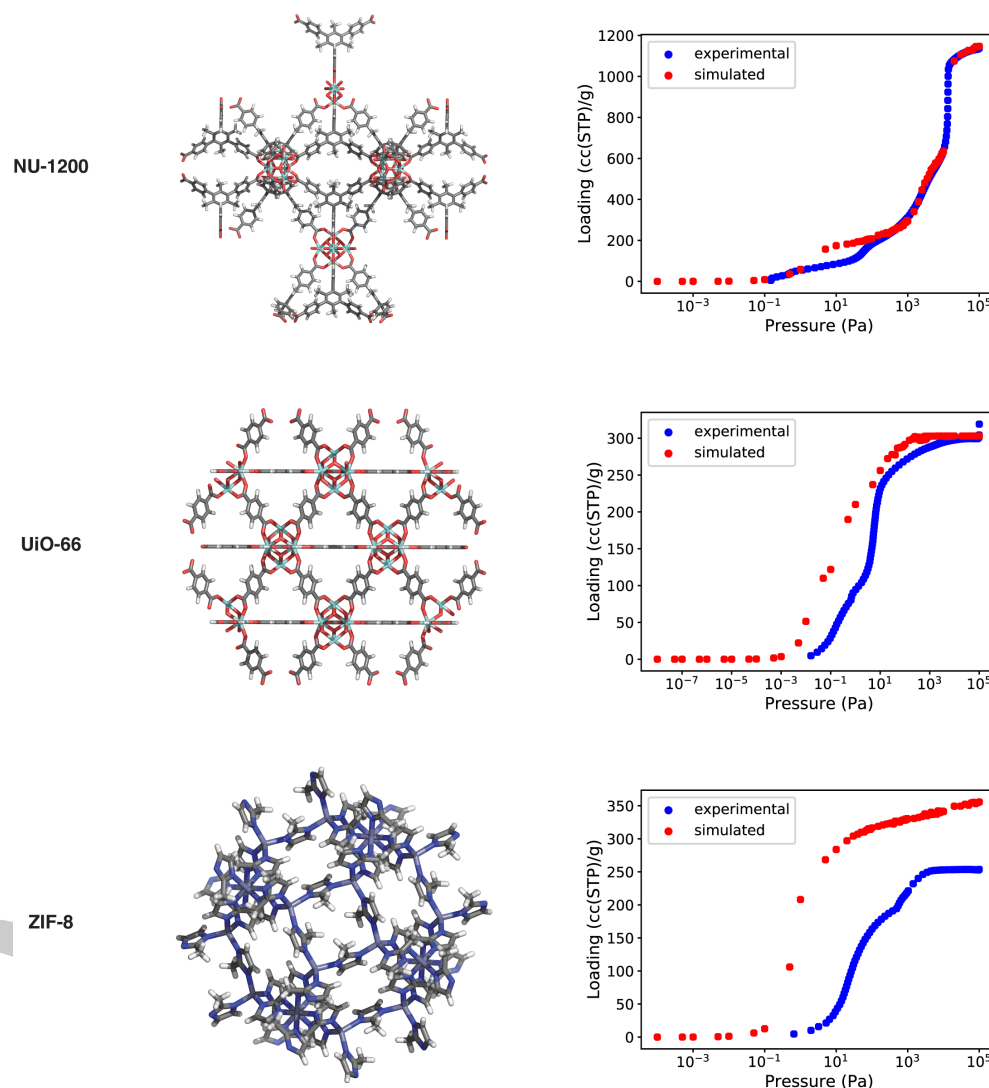


Figure 2: The crystal structures and isotherms of 3 of the 14 metal-organic frameworks used to benchmark different isotherm to surface area codes.

82 We find that over the set of 13 GCMC isotherms, the SESAMI machine learning model
83 and BEaTmap have the best correlation with Zeo++ surface areas (Willems et al., 2012)
84 calculated with a 1.67 Å probe N₂ molecule (Tables 2 and 1). Nevertheless, all software
85 are in generally good agreement, underscoring the benefit of a computational approach to
86 surface area calculation. The agreement between software is also not surprising due to the
87 similar approach taken by most of the codes of considering multiple subsets of consecutive
88 data points and applying checks like the Rouquerol criteria to select a linear region for BET
89 analysis. Indeed, this agreement is also observed over the 9 experimental isotherms (Table 3).
90 The benchmark isotherms, XLSX files of surface area predictions across different software tools
91 for both GCMC and experimental isotherms, details about settings used for each software,
92 and employed analysis scripts are available at https://github.com/hjkgrp/SESAMI_web.

Table 1: Calculated surface areas (m^2/g) for the 13 MOFs with GCMC isotherms. Cases where a software does not find a surface area are denoted by N/A. Zeo++ calculations were conducted with the same CIF files used to generate GCMC isotherms, and a 1.67 Å probe N_2 molecule, the high accuracy flag, and 2,000 samples were used. All other software took as input the GCMC isotherms.

	SESAMI 1 (BET)	SESAMI 1 (BET+ESW)	SESAMI 2 (LASSO)	BETSI	py- GAPS	BEaTmap	Zeo++
HKUST-1	2001	1933	2089	1962	1902	1980	2397
IRMOF-1	3502	3543	3123	3519	3504	N/A	3722
MIL-100 (Cr)	2107	1853	2111	N/A	1852	2094	1957
MIL-100 (Fe)	2386	2438	2203	2426	82	2423	1933
MIL-101	3828	2862	2944	N/A	2939	3331	3164
MIL-53 (Al)	1221	1168	1405	1164	1183	1212	1510
MOF-74 (Mg)	1828	1834	1902	N/A	1839	1791	1796
MOF-808	44	N/A	1275	N/A	N/A	1147	1690
NU-1000	2439	2181	2633	N/A	2144	2672	3050
NU-1200	2711	934	2601	N/A	1073	2930	3192
NU-1500 (Fe)	3543	3594	3111	N/A	3758	3492	3944
UiO-66	1239	1239	1443	N/A	1242	1304	1289
ZIF-8	1429	1386	1575	1381	1390	1414	1588

Table 2: Comparison between surface area predictions from Zeo++ and software for isotherm to surface area calculation, over the 13 MOFs with GCMC isotherms. The number of successful isotherm to surface area calculations for each software are indicated as well.

Surface area calculation software	Mean Absolute Percent Error (MAPE)	Pearson correlation coefficient	Successful calculations
SESAMI 1 (BET)	19.4	0.85	13
SESAMI 1 (BET+ESW)	17.9	0.72	12
SESAMI 2 (LASSO)	12.4	0.95	13
BETSI	17.0	0.92	5
pyGAPS	23.0	0.75	12
BEaTmap	12.6	0.93	12

Table 3: Calculated surface areas (m^2/g) for the 9 MOFs with experimental isotherms. Cases where a software does not find a surface area are denoted by N/A. All other software took as input the experimental isotherms.

	SESAMI 1 (BET)	SESAMI 1 (BET+ESW)	SESAMI 2 (LASSO)	BETSI	py- GAPS	BEaTmap
HKUST-1	1505	1466	1668	N/A	1495	1498
MOF-74 (Mg)	1580	1467	1692	N/A	1574	1565
MOF-808	1998	900	1727	N/A	2439	1752
NU-1000	2154	2090	2385	N/A	2654	2459
NU-1200	2893	2718	2781	2758	3917	3069

	SESAMI 1 (BET)	SESAMI 1 (BET+ESW)	SESAMI 2 (LASSO)	BETSI	py- GAPS	BEaTmap
NU-1500 (Fe)	3305	3409	2809	N/A	3413	3227
SIFSIX-3 (Ni)	356	201	716	N/A	355	353
UiO-66	1251	1228	1413	1250	1249	1246
ZIF-8	1092	910	1214	N/A	1082	1047

Acknowledgements

This publication was made possible by the generous support of the Government of Portugal through the Portuguese Foundation for International Cooperation in Science, Technology and Higher Education and was undertaken in the MIT Portugal Program. Software and website development was supported by the Office of Naval Research under grant number N00014-20-1-2150, as well as by the National Research Foundation of Korea (NRF) under grant number 2020R1C1C1010373 funded by the government of Korea (MSIT). We thank Timur Islamoglu, Karam Idrees, and Omar Farha for kindly providing the raw data of the experimental isotherms in the work by Islamoglu et al. (2022).

References

- Brunauer, S., Emmett, P. H., & Teller, E. (1938). Adsorption of Gases in Multimolecular Layers. *Journal of the American Chemical Society*, 60(2), 309–319. <https://doi.org/10.1021/ja01269a023>
- Datar, A., Chung, Y. G., & Lin, L. (2020). Beyond the BET Analysis: The Surface Area Prediction of Nanoporous Materials Using a Machine Learning Method. *The Journal of Physical Chemistry Letters*, 11. <https://doi.org/10.1021/acs.jpclett.0c01518>
- Dubbeldam, D., Calero, S., Ellis, D. E., & Snurr, R. Q. (2016). RASPA: Molecular Simulation Software for Adsorption and Diffusion in Flexible Nanoporous Materials. *Molecular Simulation*, 42(2), 81–101. <https://doi.org/10.1080/08927022.2015.1010082>
- Fagerlund, G. (1973). Determination of Specific Surface by the BET Method. *Matériaux Et Construction*, 6, 239–245. <https://doi.org/10.1007/BF02479039>
- Gómez-Gualdrón, D. A., Moghadam, P. Z., Hupp, J. T., Farha, O. K., & Snurr, R. Q. (2016). Application of Consistency Criteria to Calculate BET Areas of Micro- and Mesoporous Metal–Organic Frameworks. *Journal of the American Chemical Society*, 138(1), 215–224. <https://doi.org/10.1021/jacs.5b10266>
- Iacomì, P. (2019). *pyGAPS 4.4.0 documentation*. Sphinx. <https://pygaps.readthedocs.io/en/master/>
- Iacomì, P., & Llewellyn, P. L. (2019). pyGAPS: a Python-Based Framework for Adsorption Isotherm Processing and Material Characterisation. *Adsorption*, 25. <https://doi.org/10.1007/s10450-019-00168-5>
- Islamoglu, T., Idrees, K. B., Son, F. A., Chen, Z., Lee, S.-J., Li, P., & Farha, O. K. (2022). Are You Using the Right Probe Molecules for Assessing the Textural Properties of Metal–Organic Frameworks? *Journal of Materials Chemistry A*, 10(1), 157–173. <https://doi.org/10.1039/D1TA08021K>
- Osterrieth, J. W. M., Rampersad, J., Madden, D., Rampal, N., Skoric, L., Connolly, B., Allendorf, M. D., Stavila, V., Snider, J. L., Ameloot, R., & others. (2022). How

- 129 Reproducible are Surface Areas Calculated from the BET Equation? *Advanced Materials*,
130 34. <https://doi.org/10.1002/adma.202201502>
- 131 Rampersad, J., Osterrieth, J. W., & Rampal, N. (2020). *Betsi-gui*. GitHub. <https://github.com/nakulrampal/betsi-gui>
- 132
- 133 Rouquerol, J., Llewellyn, P., Rouquerol, F., & others. (2007). Is the BET Equation Applicable
134 to Microporous Adsorbents? *Stud. Surf. Sci. Catal*, 160(07), 49–56.
- 135 Rouquerol, Jean, Rouquerol, F., Llewellyn, P., Maurin, G., & Sing, K. S. (2013). *Adsorption*
136 *by Powders and Porous Solids: Principles, Methodology and Applications*. Academic press.
137 <https://doi.org/10.1016/B978-0-12-598920-6.X5000-3>
- 138 Sadeghi, A., Bell, E., & Gostick, J. (2020). *Beatmap v0.1.2*. GitHub. <https://github.com/PMEAL/beatmap>
- 139
- 140 Sinha, P., Datar, A., Jeong, C., Deng, X., Chung, Y. G., & Lin, L. (2019). Surface Area
141 Determination of Porous Materials Using the Brunauer–Emmett–Teller (BET) Method:
142 Limitations and Improvements. *The Journal of Physical Chemistry C*, 123. <https://doi.org/10.1021/acs.jpcc.9b02116>
- 143
- 144 Wang, T. C., Bury, W., Gómez-Gualdrón, D. A., Vermeulen, N. A., Mondloch, J. E., Deria, P.,
145 Zhang, K., Moghadam, P. Z., Sarjeant, A. A., Snurr, R. Q., & others. (2015). Ultrahigh
146 Surface Area Zirconium MOFs and Insights into the Applicability of the BET Theory.
147 *Journal of the American Chemical Society*, 137(10), 3585–3591. <https://doi.org/10.1021/ja512973b>
- 148
- 149 Willems, T. F., Rycroft, C. H., Kazi, M., Meza, J. C., & Haranczyk, M. (2012). Algorithms
150 and Tools for High-Throughput Geometry-Based Analysis of Crystalline Porous Materials.
151 *Microporous and Mesoporous Materials*, 149(1), 134–141. <https://doi.org/10.1016/j.micromeso.2011.08.020>
- 152